

Effects of Ca on Tensile Properties and Stretch Formability at Room Temperature in Mg-Zn and Mg-Al Alloys

Yasumasa Chino¹, Takamichi Ueda², Yuki Otomatsu², Kensuke Sassa¹,
Xinsheng Huang¹, Kazutaka Suzuki¹ and Mamoru Mabuchi²

¹Materials Research Institute for Sustainable Development, National Institute of Advanced Industrial Science and Technology, Nagoya 463-8560, Japan

²Department of Energy Science and Technology, Graduate School of Energy Science, Kyoto University, Kyoto 606-8501, Japan

The tensile tests and the Erichsen tests at room temperature have been performed on seven kinds of Mg alloys: Mg-1.5Zn, Mg-1.5Zn-0.1Ca, Mg-3Zn, Mg-3Zn-0.1Ca, Mg-3Al, Mg-3Al-0.1Ca and Mg-1Al-1Zn-0.1Ca-0.5Mn alloys. In the Mg-Zn alloys, the 0.2% proof stress at 90°, which was the angle between the tensile direction and the RD, was decreased by addition of Ca, while the 0.2% proof stress at 0° was increased by addition of Ca. Also, an increase in elongation to failure by addition of Ca at 90° was larger than that at 0°. However, such variations in tensile properties by addition of Ca were not found in the Mg-Al alloy. The stretch formability for the Mg-Zn alloys was significantly enhanced by addition of Ca, while the stretch formability of the Mg-Al alloy was not enhanced by addition of Ca. These results by the mechanical testing are ascribed to the variations in basal texture by addition of Ca. [doi:10.2320/matertrans.M2011048]

(Received February 3, 2011; Accepted April 19, 2011; Published June 8, 2011)

Keywords: magnesium alloy, tensile properties, stretch formability, texture, rolling

1. Introduction

Alloying generally strengthens metallic materials because movement of dislocations is retarded by interactions with solute atoms in solid-solution alloys. However, there is a trade-off relation between the strength and the ductility, and the formability is often reduced by alloying. However, it has been recently reported that addition of specific elements such as Ce, Y and Ca give rise to a significant enhancement in stretch formability at room temperature in Mg alloys.^{1–10)} For example, Mg-1.5 mass%Zn-0.1 mass%Ca alloy exhibited a large Erichsen value of 8.2 at room temperature.⁵⁾ This value is comparable with the stretch formability of commercial wrought aluminum alloys.¹¹⁾ In general, because the critical resolved shear stresses for non-basal slips are much larger than that for the basal slip^{12,13)} and the non-basal slips hardly occurs at room temperature in Mg based materials, they exhibit poor plastic formability at room temperature. The finding of enhanced stretch formability at room temperature in the Mg alloys is attractive for commercial applications. In particular, the Mg-Zn-Ca alloy is most desirable because Ca is abundant resources in the earth's crust (high Clarke number) and available throughout the world.

The elongation to failure can be enhanced by the grain size refinement in Mg.^{14,15)} However, the stretch formability at room temperature more strongly depends on the (0002) texture than the grain size.^{16,17)} Hence, the enhanced stretch formability by the addition of the specific elements is attributed to the unique basal texture: a reduction in basal texture intensity and a tilt of the basal poles to the TD.^{2,3,5,6,8,10,18,19)} A recent work¹⁰⁾ showed that the addition of Ca in Mg-Zn alloy gave rise to the formation of the unique texture, while the unique basal texture was not formed by addition of Ca in pure Mg. Thus, effects of Ca are complicated. However, there are too few data to understand the effects of Ca, and furthermore researches are needed.

In the present work, tensile tests and Erichsen tests at room temperature are performed on the Mg alloys: Mg-Zn, Mg-Zn-Ca, Mg-Al, Mg-Al-Ca, Mg-Al-Zn-Ca-Mn alloys to compare effects of Ca on the tensile properties and stretch formability of Mg-Zn alloy with those of Mg-Al alloy.

2. Experimental Procedure

Extrusions of Mg-1.5 mass%Zn (Mg-1.5Zn) alloy, Mg-1.5 mass%Zn-0.07 mass%Ca (Mg-1.5Zn-0.1Ca) alloy, Mg-3.0 mass%Zn (Mg-3Zn) alloy, Mg-3.0 mass%Zn-0.12 mass%Ca (Mg-3Zn-0.1Ca) alloy, Mg-2.9 mass%Al (Mg-3Al) alloy, Mg-2.9 mass%Al-0.11 mass%Ca (Mg-3Al-0.1Ca) alloy and Mg-1.4 mass%Al-0.9 mass%Zn-0.09 mass%Ca-0.7 mass%Mn (Mg-1Al-1Zn-0.1Ca-0.5Mn) alloy were prepared. After the alloys were heated in a furnace, unidirectional rolling was performed at a rolling reduction of 20%. The heating temperature was 723 K for the Mg-1.5Zn, Mg-1.5Zn-0.1Ca, Mg-3Al and Mg-3Al-0.1Ca alloys, 743 K for the Mg-1Zn-1Al-0.1Ca-0.5Mn alloy and 623 K for the Mg-3Zn and Mg-3Zn-0.1Ca alloys, respectively. The heating and rolling treatments were repeated, and the alloys were rolled to a thickness of 1 mm. The rolling direction was perpendicular to the extrusion direction. Finally, the rolled alloys were annealed at 623 K for 5.4×10^3 s.

The microstructures of the rolled and subsequently annealed Mg alloys and the as-rolled Mg alloys were investigated by optical microscopy. The grain size of the specimens was determined by the intercept method.²⁰⁾ The (0002) plane pole figure of the rolled and subsequently annealed Mg alloys and the as-rolled Mg alloys at the center through a thickness was investigated by Schulz reflection method. The data was normalized using powder Mg data.

Tensile specimens with 10 mm gage length, 5 mm gage width and 1 mm gage thickness were machined from the rolled and subsequently annealed Mg alloys. Tensile tests were carried out with an initial strain rate of 1.7×10^{-3} s⁻¹,

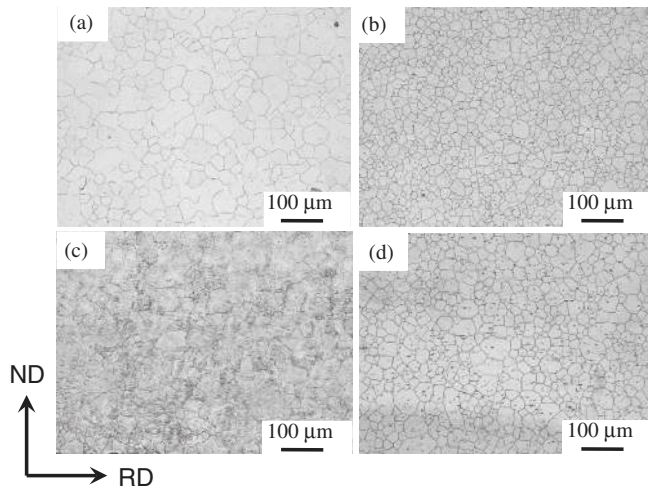


Fig. 1 Microstructures of the rolled and subsequently annealed Mg-Zn and Mg-Zn-Ca alloys: (a) the Mg-1.5Zn alloy, (b) the Mg-1.5Zn-0.1Ca alloy, (c) the Mg-3Zn alloy and (d) the Mg-3Zn-0.1Ca alloy.

where the angle between the tensile direction and the RD was set to 0, 45 and 90°. Dislocations in the Mg-1.5Zn-0.1Ca alloy tensile-deformed to 1%, where the angle between the tensile direction and the RD was set to 90°, were observed by Transmission Electron Microscope (TEM). The incident beam direction was set parallel to either the $[01\bar{1}0]$ direction or the $[\bar{2}110]$ direction.

A circular blank with a diameter of 60 mm was machined from the rolled and subsequently annealed specimens. Erichsen tests using a hemispherical punch with a diameter of 20 mm were carried out at room temperature to investigate the stretch formability of the specimens, and Erichsen value (IE), which was the punch stroke at fracture initiation, was measured. The punch speed and blank holder force were 5 mm/min and 10 kN, respectively. Graphite grease was used as the lubricant.

3. Results

3.1 Microstructure

Microstructures of the rolled and subsequently annealed Mg-Zn and Mg-Zn-Ca alloys are shown in Fig. 1, where (a) is the Mg-1.5Zn alloy, (b) is the Mg-1.5Zn-0.1Ca alloy, (c) is the Mg-3Zn alloy and (d) is the Mg-3Zn-0.1Ca alloy. The grains were almost equiaxed in the Mg alloys. The grain size was 63 μm for the Mg-1.5Zn alloy, 32 μm for the Mg-1.5Zn-0.1Ca alloy, 56 μm for the Mg-3Zn alloy and 40 μm for the Mg-3Zn-0.1Ca alloy, respectively. The grain sizes for the Mg-Zn-Ca alloys were smaller than those for the Mg-Zn alloys. On the other hand, there was a minor effect of Zn concentration on the grain size.

Microstructures of the rolled and subsequently annealed Mg-Al, Mg-Al-Ca and Mg-Al-Zn-Ca-Mn alloys are shown in Fig. 2, where (a) is the Mg-3Al alloy, (b) is the Mg-3Al-0.1Ca alloy and (c) is the Mg-1Al-1Zn-0.1Ca-0.5Mn alloy. The grains were almost equiaxed in the Mg alloys. The grain size was 60 μm for the Mg-3Al alloy, 30 μm for the Mg-3Al-0.1Ca alloy and 19 μm for the Mg-1Al-1Zn-0.1Ca-0.5Mn alloy, respectively. The grain size of the Mg-1Al-1Zn-0.1Ca-

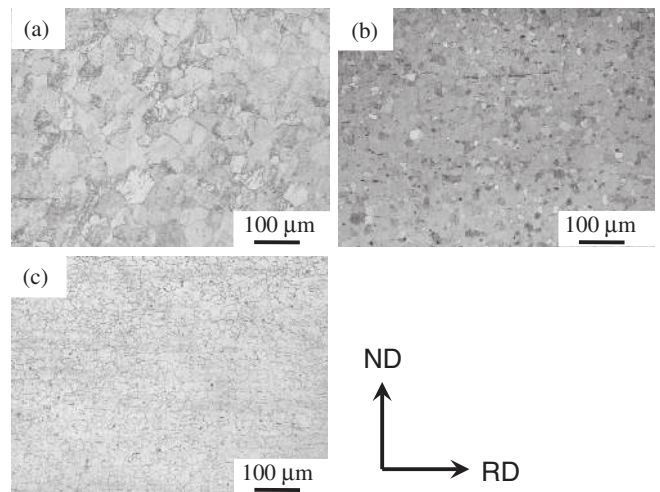


Fig. 2 Microstructures of the rolled and subsequently annealed Mg-Al, Mg-Al-Ca and Mg-Al-Zn-Ca-Mn alloys: (a) the Mg-3Al alloy, (b) the Mg-3Al-0.1Ca alloy and (c) the Mg-1Al-1Zn-0.1Ca-0.5Mn alloy.

0.5Mn alloy was the smallest in the Mg alloys investigated. This is due to precipitates of second phase particles such as Al_3Mn_5 ,²¹⁾ which effectively pin a grain growth during hot rolling, in AZ series alloys. The grain size of the Mg-Al-Ca alloy was smaller than that of the Mg-Al alloy. This trend was found in the Mg-Zn and Mg-Zn-Ca alloys, indicating that addition of Ca suppressed grain growth. Few precipitates were observed in the Mg-Zn-Ca alloy.^{5,10)} Similarly, precipitates were hardly observed in the Mg-Al-Ca alloy. In the casting process, Ca addition in Mg alloy is known to be effective for grain refinement, because segregation of Ca at the front of grain growth forms a non-negligible constitutional undercooling in a diffusion layer ahead of the advancing solid/liquid interface and then restricts the grain growth and promotes the nucleation of the primary Mg.^{22,23)} It is suggested that the segregation of solute Ca atoms in Mg alloy may suppress the grain growth not only of the solid/liquid interface but also solid/solid interface (grain boundaries). Further search is needed to understand effects of Ca on grain growth during rolling and annealing processes.

The (0002) pole figures of the rolled and subsequently annealed Mg-Zn and Mg-Zn-Ca alloys are shown in Fig. 3, where (a) is the Mg-1.5Zn alloy, (b) is the Mg-1.5Zn-0.1Ca alloy, (c) is the Mg-3Zn alloy and (d) is the Mg-3Zn-0.1Ca alloy. The intensities of basal texture for the Mg-Zn-Ca alloys were much lower than those for the Mg-Zn alloys. Clearly, addition of Ca suppressed the formation of basal texture. In addition, the basal poles were split toward the TD in the Mg-Zn-Ca alloys. On the other hand, the basal texture was intense and the level curves of texture intensity were broadened to the RD, not to the TD, in the Mg-Zn alloys. The characteristics of a reduction in basal texture intensity and a split of the basal poles to the TD were found in both the Mg-1.5Zn-0.1Ca and the Mg-3Zn-0.1Ca alloys, which was independent of the Zn concentration. The previous work¹⁰⁾ showed that the level curves of basal texture intensity were broadened to the RD in the Mg-Ca alloy containing no Zn, although the intensity of basal texture was low, where the maximum value of basal texture intensity was 5.6. Therefore,

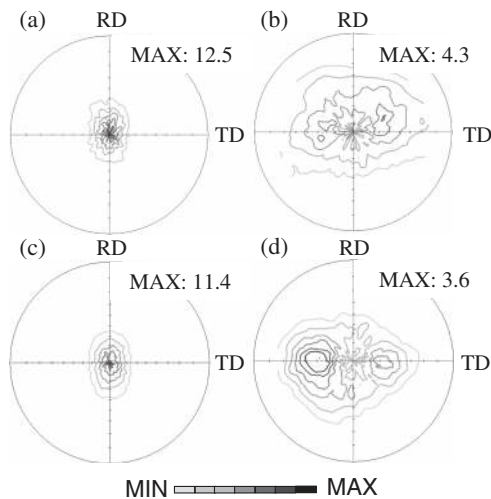


Fig. 3 The (0002) pole figures of the rolled and subsequently annealed Mg-Zn and Mg-Zn-Ca alloys: (a) the Mg-1.5Zn alloy, (b) the Mg-1.5Zn-0.1Ca alloy, (c) the Mg-3Zn alloy and (d) the Mg-3Zn-0.1Ca alloy.

it seems that Zn has an effect of tilting the basal planes to the RD, but no effect of reducing the basal texture intensity, while Ca has effects of tilting the basal planes to the RD and reducing the basal texture intensity. It is noted that the basal poles were split to the TD by the addition of both Ca and Zn, although the basal planes tended to be tilted to the RD by the addition of either Ca or Zn. The split of basal poles to the TD was more prominent in the Mg-3Zn-0.1Ca alloy than in the Mg-1.5Zn-0.1Ca alloy. Therefore, it is suggested that an interaction of Ca and Zn atoms plays an important role in splitting of basal poles to the TD. The basal poles were split to the TD in the Mg-Zn-Ce alloy,²⁾ while they were split to the RD in the Mg-Ce alloy.²⁴⁾ The trends for the Mg-Ce and Mg-Zn-Ce alloys are the same as those for the Mg-Ca and Mg-Zn-Ca alloys.

The (0002) pole figures of the rolled and subsequently annealed Mg-Al, Mg-Al-Ca and Mg-Al-Zn-Ca-Mn alloys are shown in Fig. 4, where (a) is the Mg-3Al alloy, (b) is the Mg-3Al-0.1Ca alloy and (c) is the Mg-1Al-1Zn-0.1Ca-0.5Mn alloy. The basal texture was intense and the level curves of texture intensity were broadened to the RD in the Mg-Al alloy, indicating that Al has an effect of tilting the basal planes to the RD, but no effect of reducing the basal texture intensity. These effects of Al are the same as those of Zn. The intensity of basal texture for the Mg-Al-Ca alloy was lower than that for the Mg-Al alloy. However, a reduction in basal texture intensity by addition of Ca was lower in the Mg-Al alloy than in the Mg-Zn alloys. In addition, the basal planes were tilted toward the RD in the Mg-Al-Ca alloy. Therefore, it is suggested that tilting of basal planes to the TD is induced by an interaction of Ca and Zn atoms, not by an interaction of the Ca and Al atoms. It is noted that an interaction between solute atoms is crucial in tilting the basal planes to the TD.

3.2 Tensile properties

The nominal stress–nominal strain curves at 0, 45 and 90° for the rolled and subsequently annealed Mg-Zn and Mg-Zn-Ca alloys are shown in Fig. 5, where (a) is the Mg-1.5Zn

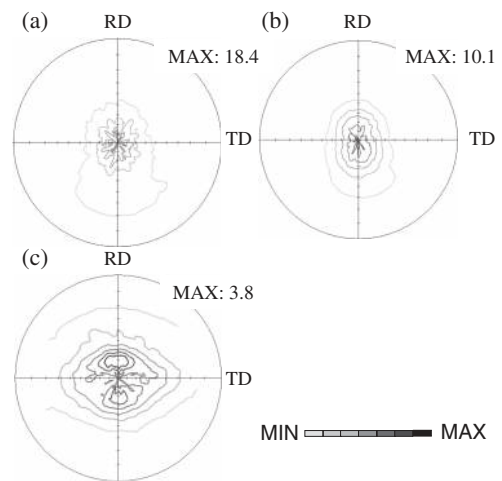


Fig. 4 The (0002) pole figures of the rolled and subsequently annealed Mg-Al, Mg-Al-Ca and Mg-Al-Zn-Ca-Mn alloys: (a) the Mg-3Al alloy, (b) the Mg-3Al-0.1Ca alloy and (c) the Mg-1Al-1Zn-0.1Ca-0.5Mn alloy.

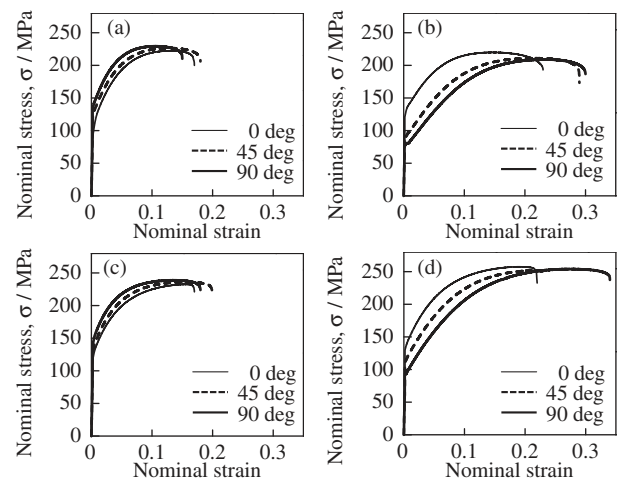


Fig. 5 The nominal stress–nominal strain curves at 0, 45 and 90° for the rolled and subsequently annealed Mg-Zn and Mg-Zn-Ca alloys, (a) the Mg-1.5Zn alloy, (b) the Mg-1.5Zn-0.1Ca alloy, (c) the Mg-3Zn alloy and (d) the Mg-3Zn-0.1Ca alloy.

alloy, (b) is the Mg-1.5Zn-0.1Ca alloy, (c) is the Mg-3Zn alloy and (d) is the Mg-3Zn-0.1Ca alloy. The lowest 0.2% proof stress was found at 0° and the largest one was found at 90° for the Mg-Zn alloys. The 0.2% proof stress at 0° was increased by addition of Ca, but the 0.2% proof stresses at 45 and 90° were decreased by addition of Ca. A decrease in 0.2% proof stress by addition of Ca was larger at 90° than at 45°. As a result, the lowest 0.2% proof stress was found at 90° and the largest one was found at 0° for the Mg-Zn-Ca alloys. The variations in 0.2% proof stress by addition of Ca correspond to tilting of the basal planes to the TD by addition of Ca. The elongation to failure was increased by addition of Ca, independently of the tensile directions. An increase in elongation to failure by addition of Ca at 90° was larger than those at 0 and 45°. This also corresponds to tilting of the basal planes to the TD by addition of Ca.

The nominal stress–nominal strain curves at 0, 45 and 90° for the rolled and subsequently annealed Mg-Al, Mg-Al-Ca and Mg-Al-Zn-Ca-Mn alloys are shown in Fig. 6, where (a)

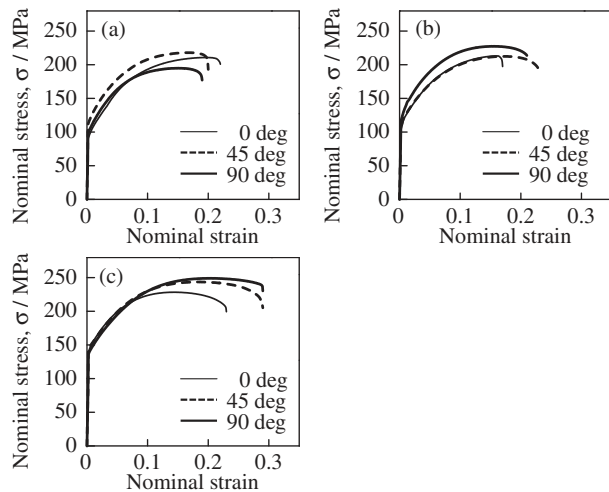


Fig. 6 The nominal stress–nominal strain curves at 0, 45 and 90° for the rolled and subsequently annealed Mg-Al, Mg-Al-Ca and Mg-Al-Zn-Ca-Mn alloys, (a) the Mg-3Al alloy, (b) the Mg-3Al-0.1Ca alloy and (c) the Mg-1Al-1Zn-0.1Ca-0.5Mn alloy.

is the Mg-3Al alloy, (b) is the Mg-3Al-0.1Ca alloy and (c) is the Mg-1Al-1Zn-0.1Ca-0.5Mn alloy. As shown in Fig. 5, the tensile properties were significantly varied by addition of Ca in the Mg-Zn alloys. However, such large variations in tensile properties by addition of Ca were not found in Mg-Al alloy. This is because a reduction in basal texture intensity by addition of Ca was lower in the Mg-Al alloy than in the Mg-Zn alloys and the basal planes were not tilted toward the TD in the Mg-Al-Ca alloy.

3.3 Stretch formability

The specimens after the Erichsen tests at room temperature for the rolled and subsequently annealed Mg-Zn and Mg-Zn-Ca alloys are shown in Fig. 7, where (a) is the Mg-1.5Zn alloy, (b) is the Mg-1.5Zn-0.1Ca alloy, (c) is the Mg-3Zn alloy and (d) is the Mg-3Zn-0.1Ca alloy. The Erichsen value was 3.4 for the Mg-1.5Zn alloy, 8.2 for the Mg-1.5Zn-0.1Ca alloy, 4.1 for the Mg-3Zn alloy and 8.1 for the Mg-3Zn-0.1Ca alloy, respectively. The stretch formability for the Mg-Zn alloys was significantly enhanced by addition of Ca. The Erichsen values of the Mg-Zn-Ca alloys are comparable with those of commercial Al alloys.¹¹⁾ An enhanced stretch formability of the Mg-Zn-Ca alloys are closely related to the texture softening originating from the weakening of basal texture intensity and the splitting of basal pole toward the TD. It is suggested that an enhancement in stretch formability by addition of Ca was independent of the Zn concentrations, at least in the range investigated.

The specimens after the Erichsen tests at room temperature for the rolled and subsequently annealed Mg-Al, Mg-Al-Ca and Mg-Al-Zn-Ca-Mn alloys are shown in Fig. 8, where (a) is the Mg-3Al alloy, (b) is the Mg-3Al-0.1Ca alloy and (c) is the Mg-1Al-1Zn-0.1Ca-0.5Mn alloy. The Erichsen value was 5.6 for the Mg-3Al alloy, 6.5 for the Mg-3Al-0.1Ca alloy and 7.6 for the Mg-1Al-1Zn-0.1Ca-0.5Mn alloy, respectively. The stretch formability of the Mg-Al alloy was not significantly enhanced by addition of Ca. This corresponds to the minor variation in basal texture by addition of Ca in the Mg-Al alloy.

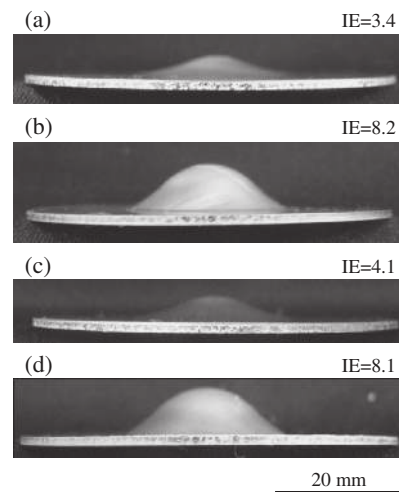


Fig. 7 The specimens after the Erichsen tests at room temperature for the rolled and subsequently annealed Mg-Zn and Mg-Zn-Ca alloys: (a) the Mg-1.5Zn alloy, (b) the Mg-1.5Zn-0.1Ca alloy, (c) the Mg-3Zn alloy and (d) the Mg-3Zn-0.1Ca alloy.

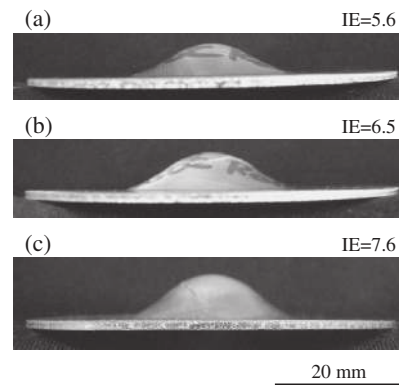


Fig. 8 The specimens after the Erichsen tests at room temperature for the rolled and subsequently annealed Mg-Al, Mg-Al-Ca and Mg-Al-Zn-Ca-Mn alloys: (a) the Mg-3Al alloy, (b) the Mg-3Al-0.1Ca alloy and (c) the Mg-1Al-1Zn-0.1Ca-0.5Mn alloy.

4. Discussion

The previous study has revealed that the basal planes of the rolled Mg alloy tend to be tilted to the RD by addition of only Ca.¹⁰⁾ The tilting of the basal planes to the RD is also observed in hot-deformed Mg with dilute Y addition.²⁵⁾ Agnew *et al.*²⁵⁾ suggested that the splitting of basal planes to the RD is related to the enhanced $\langle c + a \rangle$ slip. The other previous studies²⁶⁾ suggested that the tilting of basal planes to the RD is because of the secondary $\{10\bar{1}2\}$ twinning within primary $\{10\bar{1}1\}$ compression twins. Figure 9 shows microstructures of the as-rolled Mg-1.5Zn, Mg-1.5Zn-0.1Ca, Mg-3Al and Mg-3Al-0.1Ca alloys. Many deformation twins are observed in all the alloys. It seems that the Mg alloys without Ca addition exhibited more extensive twinning compared with Mg alloys with Ca. This is due to smaller grain size of the Mg alloys with Ca.¹⁵⁾ The suppression of twinning by addition of Ca in Mg alloys indicates that twinning is not likely related to the tilting of basal planes to the RD. The (0002) plane pole figures of the as-rolled Mg-3Al and Mg-3Al-0.1Ca alloys are shown in Fig. 10(c) and (d). The

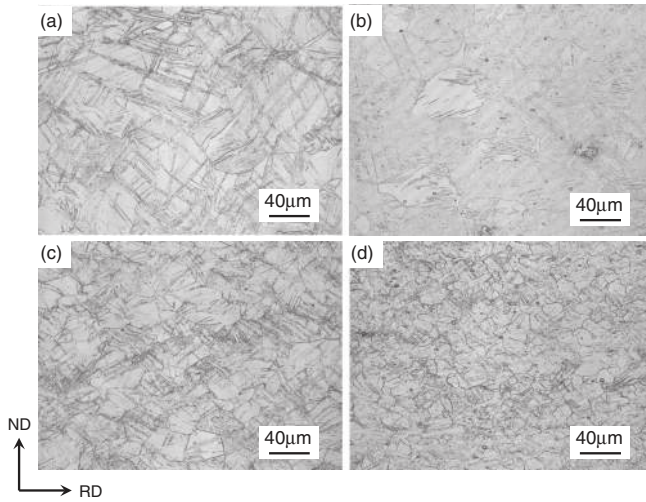


Fig. 9 Microstructures of the as-rolled Mg alloys: (a) the Mg-1.5Zn alloy, (b) the Mg-1.5Zn-0.1Ca alloy, (c) the Mg-3Al alloy and (d) the Mg-3Al-0.1Ca alloy.

intensity of basal plane texture was reduced by the Ca addition in the same manner as the rolled and subsequently annealed alloys as shown in Fig. 4. It is noted that the tilting of basal planes to the RD in Mg-3Al-0.1Ca alloy was more pronounced compared with that in Mg-3Al alloy. Sandlöbes *et al.*²⁷⁾ investigated the dislocation motion in the Mg-3 mass%Y alloy deformed at room temperature, and reported that activity of $\langle c + a \rangle$ slips are significantly enhanced by Y addition compared with those of pure Mg. Therefore, the tilt of basal planes to the RD in Mg with dilute Ca addition is also suggested to be due to an activation of the pyramidal $\langle c + a \rangle$ and/or prismatic $\langle c \rangle$ slips.

The (0002) plane pole figures of the as-rolled Mg-1.5Zn and Mg-1.5Zn-0.1Ca alloys are shown in Fig. 10(a) and (b). The as-rolled Mg-1.5Zn alloy had almost the same texture as that of the annealed specimen. On the other hand, the clear splitting of basal poles to the TD observed in the rolled and subsequently annealed Mg-1.5Zn-0.1Ca alloy was not observed in the as-rolled Mg-1.5Zn-0.1Ca alloy, indicating that microstructural changes during annealing such as static recrystallization pronounced the splitting of basal planes to the TD. However, it should be noted that the basal planes of the as-rolled Mg-1.5Zn-0.1Ca alloy exhibited much broader distribution to the TD compared with the as-rolled Mg-1.5Zn alloy. This result implies that the tilting of basal planes to the TD occurred not only during annealing but also during rolling. The experimental results showed that the basal planes were split to the TD only in the Mg-(Al)-Zn-Ca alloys. The split to TD indicates that the prismatic $\langle a \rangle$ slip occurs easily during rolling.²⁸⁾ It was reported in the previous work³⁾ that the quadruple basal poles were formed by addition of Y in Mg-Zn alloys, suggesting that not only the prismatic $\langle a \rangle$ slip, but also the pyramidal $\langle c + a \rangle$ or prismatic $\langle c \rangle$ slip occur. Figure 11 shows the transmission electron micrographs of the Mg-1.5Zn-0.1Ca alloy specimen deformed to 1%, where all dislocations are visible in (a), dislocations having the $\langle a \rangle$ Burgers vector are out of contrast in (b) and dislocations having the $\langle c \rangle$ Burgers vector are out of contrast in (c). In

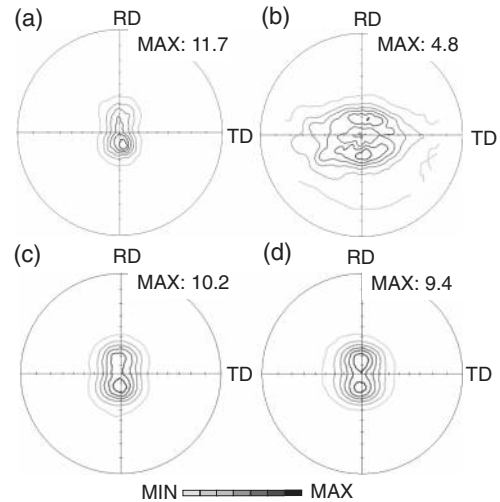


Fig. 10 The (0002) pole figures of the as-rolled Mg alloys: (a) the Mg-1.5Zn alloy, (b) the Mg-1.5Zn-0.1Ca alloy, (c) the Mg-3Al alloy and (d) the Mg-3Al-0.1Ca alloy.

the figures, the TD-ND plane was observed. For example, in the white circles, the dislocations were visible in (b), but not (c), indicating that the dislocation had the $\langle c \rangle$ Burgers vector. This fact indicates that the prismatic $\langle c \rangle$ slip was induced in the Mg-Zn-Ca alloys. Therefore, it is suggested that both the prismatic $\langle a \rangle$ and $\langle c \rangle$ slips occur in the Mg-Zn-Ca alloy, promoting a splitting of basal plane toward the TD during rolling. The reason why quadruple basal poles were not found in the Mg-Zn-Ca alloys is probably that the Ca content was low.

In the Mg-Al-Ca alloy, no split of basal poles to the TD was found. This indicates that the prismatic $\langle a \rangle$ slip was not induced by addition of Ca in the Mg-Al alloy. Both the prismatic $\langle a \rangle$ and $\langle c \rangle$ (or pyramidal $\langle c + a \rangle$) slips are likely required to promote the texture with a splitting of basal plane toward the TD. The experimental results in the present work suggested that these slips are enhanced by an interaction of Zn and Ca atoms, but neither by addition of sole element nor by an interaction of Al and Ca atoms.

In general, since the $\langle c + a \rangle$ and/or $\langle c \rangle$ slips induce the straining to the thickness direction of the rolled Mg alloy, the stretch formability can be enhanced even when the basal planes are aligned parallel to the rolling plane. However, the main contribution to straining in stretch forming is the basal $\langle a \rangle$ slip, whose slip systems are only two.^{12,13)} The edge dislocations cannot move through cross-slipping. Hence, the screw dislocations play a dominant role in straining although the prismatic $\langle a \rangle$ slip is required for cross-slipping. Therefore, the stretch formability cannot be enhanced without the prismatic $\langle a \rangle$ slip even when the $\langle c + a \rangle$ and $\langle c \rangle$ slips are induced by addition of Ca. The TEM observation revealed that an addition of Ca in Mg-Zn alloys promoted prismatic $\langle a \rangle$ and $\langle c \rangle$ slips at even room temperature. This fact indicates that not only texture softening but also solid solution softening¹⁰⁾ caused by an activation of prismatic $\langle a \rangle$ and $\langle c \rangle$ slips contributes to an enhancement of stretch formability of Mg-Zn-Ca alloy. The c/a ratio was 1.6249 and 1.6242 for the Mg-1.5Zn and the Mg-1.5Zn-0.1Ca alloys, and 1.6246 and 1.6250 for the Mg-3Al and the Mg-3Al-0.1Ca alloys,

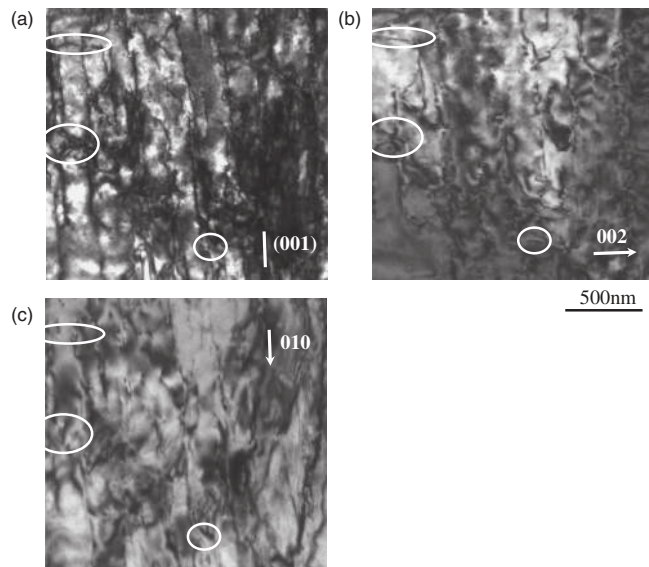


Fig. 11 The transmission electron micrographs of the Mg-1.5Zn-0.1Ca alloy specimen tensile-deformed to 1%, where all dislocations are visible in (a), dislocations having the (a) Burgers vector are out of contrast in (b) and dislocations having the (c) Burgers vector are out of contrast in (c). The tensile direction and the RD was set to 90°. In the figures, the TD-ND plane is observed, and typical dislocations with (c) Burgers vector were marked by the white circles.

respectively. Thus, the c/a ratio was not changed by addition of Ca and effects of an interaction of solute atoms could not be explained from the viewpoint of the c/a ratio. The first principles calculations are in progress to understand effects of an interaction of solute atoms on dislocation movement in the slip systems.

5. Conclusions

The tensile tests and the Erichsen tests at room temperature were performed on seven kinds of Mg alloys: Mg-1.5Zn, Mg-1.5Zn-0.1Ca, Mg-3Zn, Mg-3Zn-0.1Ca, Mg-3Al, Mg-3Al-0.1Ca and Mg-1Al-1Zn-0.1Ca-0.5Mn alloys. The results are concluded as follows.

- (1) The intensities of basal texture for the Mg-Zn-Ca alloys were much lower than those for the Mg-Zn alloys. In addition, the basal poles were split toward the TD in the Mg-Zn-Ca alloys. On the other hand, the basal texture was intense and the level curves of texture intensity were broadened to the RD, not to the TD, in the Mg-Zn alloys.
- (2) The intensity of basal texture for the Mg-Al-Ca alloy was lower than that for the Mg-Al alloy. However, a reduction in basal texture intensity by addition of Ca was lower in the Mg-Al alloy than in the Mg-Zn alloys. In addition, the basal planes were tilted toward the RD in the Mg-Al-Ca alloy.
- (3) In the Mg-Zn alloys, the 0.2% proof stresses at 45 and 90° were decreased by addition of Ca, while the 0.2% proof stress at 0° was increased by addition of Ca. A decrease in 0.2% proof stress by addition of Ca was larger at 90° than at 45°. Also, an increase in elongation to failure by addition of Ca at 90° was larger than those

at 0 and 45°. These variations in tensile properties by addition of Ca corresponded to tilting of the basal planes to the TD.

- (4) The stretch formability for the Mg-Zn alloys was significantly enhanced by addition of Ca. However, the stretch formability of the Mg-Al alloy was not enhanced by addition of Ca. These results were related to the variations in basal texture by addition of Ca.

Acknowledgement

This study was partially supported by JSPS Grant-in-Aid for Scientific Research (C) (KAKENHI, 22605007).

REFERENCES

- 1) Y. Chino, K. Sassa and M. Mabuchi: *Mater. Trans.* **49** (2008) 1710–1712.
- 2) Y. Chino, K. Sassa and M. Mabuchi: *Mater. Trans.* **49** (2008) 2916–2918.
- 3) Y. Chino, K. Sassa and M. Mabuchi: *Mater. Sci. Eng. A* **513–514** (2009) 394–400.
- 4) D. H. Kang, D. W. Kim, S. Kim, G. T. Bae, K. H. Kim and N. J. Kim: *Scr. Mater.* **61** (2009) 768–771.
- 5) Y. Chino, X. Huang, K. Suzuki and M. Mabuchi: *Mater. Trans.* **51** (2010) 818–821.
- 6) Y. Chino, X. Huang, K. Suzuki, K. Sassa and M. Mabuchi: *Mater. Sci. Eng. A* **528** (2010) 566–572.
- 7) S. Yi, J. Bohlen, F. Heinemann and D. Letzig: *Acta Mater.* **58** (2010) 592–605.
- 8) H. Yan, R. S. Chen and E. H. Han: *Mater. Sci. Eng. A* **527** (2010) 3317–3322.
- 9) C. L. Mendis, J. H. Bae, N. J. Kim and K. Hono: *Scr. Mater.* **64** (2011) 335–338.
- 10) Y. Chino, K. Sassa, X. Huang, K. Suzuki and M. Mabuchi: *J. Japan Inst. Metals* **75** (2011) 35–41.
- 11) *Aluminum Handbook*, 4th edition, (Japan Light Metal Association, Tokyo, 2000) p. 98.
- 12) H. Yoshinaga and R. Horiuchi: *Trans. JIM* **4** (1963) 1–8.
- 13) M. H. Yoo: *Metall. Trans. A* **12** (1981) 409–418.
- 14) J. A. Chapman and D. V. Wilson: *J. Inst. Metals* **92** (1962) 39–40.
- 15) J. Koike, T. Kobayashi, T. Mukai, H. Watanabe, M. Suzuki, K. Maruyama and K. Higashi: *Acta Mater.* **51** (2003) 2055–2065.
- 16) Y. Chino, H. Iwasaki and M. Mabuchi: *Mater. Sci. Eng.* **466** (2007) 90–95.
- 17) Y. Chino, K. Kimura and M. Mabuchi: *Acta Mater.* **57** (2009) 1476–1485.
- 18) L. W. F. Mackenzie and M. O. Pekguleryuz: *Scr. Mater.* **59** (2008) 665–668.
- 19) K. Hantzsche, J. Wendt, K. U. Kainer, J. Bohlen and D. Letzig: *JOM* **61** (2009) No. 8, 38–42.
- 20) A. W. Thompson: *Metallography* **28** (1972) 366–369.
- 21) T. Laser, M. R. Nürnberg, A. Janz, Ch. Hartig, D. Letzig, R. Schmid-Fetzer and R. Bormann: *Acta Mater.* **54** (2006) 3033–3041.
- 22) Y. C. Lee, A. K. Dahle and D. H. StJohn: *Metall. Mater. Trans. A* **31** (2000) 2895–2906.
- 23) E. Zhang and L. Yang: *Mater. Sci. Eng. A* **497** (2008) 111–118.
- 24) Y. Chino, M. Kado and M. Mabuchi: *Mater. Sci. Eng. A* **494** (2008) 343–349.
- 25) S. R. Agnew, M. H. Yoo and C. N. Tomé: *Acta Mater.* **49** (2001) 4277–4289.
- 26) S. L. Couling, J. F. Pashak and L. Sturkey: *Trans. ASM* **51** (1959) 94–107.
- 27) S. Sandlöbes, S. Zaefferer, I. Schestakow, S. Yi and R. Gonzalez-Martinez: *Acta Mater.* **59** (2011) 429–439.
- 28) R. A. Lebensohn, M. I. González, C. N. Tomé and A. A. Pochettino: *J. Nucl. Mater.* **229** (1996) 57–64.